48633

N73-12810

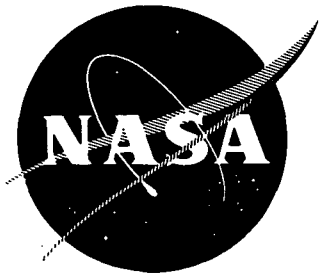

NASA CR-121033

DEVELOPMENT OF SINGLE CRYSTAL MEMBRANES

by R. W. Stormont and F. H. Cocks

TYCO LABORATORIES, INC.

prepared for

NATIONAL AERONAUTICS AND SPACE ADMINISTRATION

NASA Lewis Research Center
Contract NAS 3-15685

NOTICE

This report was prepared as an account of Government-sponsored work. Neither the United States, nor the National Aeronautics and Space Administration (NASA), nor any person acting on behalf of NASA:

A.) Makes any warranty or representation, expressed or implied, with respect to the accuracy, completeness, or usefulness of the information contained in this report, or that the use of any information, apparatus, method, or process disclosed in this report may not infringe privately-owned rights; or

B.) Assumes any liabilities with respect to the use of, or for damages resulting from the use of, any information, apparatus, method or process disclosed in this report.

As used above, "person acting on behalf of NASA" includes any employee or contractor of NASA, or employee of such contractor, to the extent that such employee or contractor of NASA or employee of such contractor prepares, disseminates, or provides access to any information pursuant to his employment or contract with NASA, or his employment with such contractor

Requests for copies of this report should be referred to

National Aeronautics and Space Administration
Scientific and Technical Information Facility
P. O. Box 33
College Park, Md. 20740

1. Report No.	2. Government Accession No.	3. Recipient's Catalog No.
NASA CR-121033		

4. Title and Subtitle	5. Report Date
DEVELOPMENT OF SINGLE CRYSTAL MEMBRANES	October 1972
	6. Performing Organization Code

7. Author(s)	8. Performing Organization Report No.
R. W. Stormont and F. H. Cocks	
	10. Work Unit No.

9. Performing Organization Name and Address	11. Contract or Grant No.
Tyco Laboratories, Inc. 16 Hickory Drive Waltham, Massachusetts 02154	NAS 3-15685
	13. Type of Report and Period Covered Final Report 6 July 1971 - 5 September 1972

12. Sponsoring Agency Name and Address	14. Sponsoring Agency Code
NASA Lewis Research Center 21000 Brookpark Road Cleveland, Ohio 44135	

15. Supplementary Notes

Project Manager: Dr. Albert C. Antoine

16. Abstract

The design and construction of a high pressure crystal growth chamber was accomplished which would allow the growth of crystals under inert gas pressures of 2 MN/m^2 (300 psi). A novel crystal growth technique called "EFG" was used to grow tubes and rods of the hollandite compounds, $BaMgTi_7O_{16}$, $K_2MgTi_7O_{16}$, and tubes of sodium beta-alumina, sodium magnesium-alumina, and potassium beta-alumina. Rods and tubes grown are characterized using metallographic and X-ray diffraction techniques. The hollandite compounds are found to be two or three-phase, composed of coarse-grained otientated crystallites. Single crystal c-axis tubes of sodium beta-alumina were grown from melts containing excess sodium oxide. Additional experiments demonstrated that crystals of magnesia doped beta-alumina and potassium beta-alumina also can be achieved by this EFG technique.

17. Key Words (Suggested by Author(s))	18. Distribution Statement
High pressure furnace Hollandite compounds Beta-alumina Single crystal membranes Batteries Crystal growth	Unlimited distribution

19. Security Classif. (of this report)	20. Security Classif. (of this page)	21. No. of Pages	22. Price*
Unclassified	Unclassified	33	

* For sale by the National Technical Information Service, Springfield, Virginia 22151

ABSTRACT

The design and construction of a high pressure crystal growth chamber was accomplished which would allow the growth of crystals under inert gas pressures of up to 2 MN/m^2. A novel crystal growth technique called "EFG" was used to grow tubes and rods of the hollandite compounds, $BaMgTi_7O_{16}$, $K_2MgTi_7O_{16}$, and tubes of sodium beta-alumina, sodium magnesium-alumina, and potassium beta-alumina. Rods and tubes grown are characterized using metallographic and X-ray diffraction techniques. The hollandite compounds are found to be two or three-phase, composed of coarse-grained orientated crystallites. Single crystal c-axis tubes of sodium beta-alumina were grown from melts containing excess sodium oxide. Additional experiments demonstrated that crystals of magnesia doped beta-alumina and potassium beta-alumina also can be achieved by this EFG technique.

Table of Contents

List of Illustrations

List of Illustrations (Continued)

List of Tables

I. SUMMARY

The objective of the present program was to grow single crystal tubes of sodium beta-alumina, sodium-magnesium beta-alumina, and certain hollandite ($BaMgTi_7O_{16}$, $K_2MgTi_7O_{16}$, $K_{1.6}Mg_{0.8}Ti_{7.2}O_{16}$) and hexatitanate ($Na_2Ti_6O_{13}$) compounds using the Tyco-developed melt growth technique known as edge-defined, film-ged growth (EFG). This technique is a modified melt-growth method which allows the growth of crystals with almost arbitrary cross-sectional shape. These materials were of interest because of their possible future application as single crystal membranes for high energy batteries.

The original program was modified after twelve months to grow rods of $K_2MgTi_7O_{16}$ instead of tubes, and to grow tubes of $K_2O \cdot 11\ Al_2O_3$ (potasium beta-alumina) instead of $Na_2Ti_6O_{13}$, as that was no longer of interest as a solid electrolyte.

Growth of the hollandite compounds was hindered by the fact that none of the compounds mentioned above were found to melt congruently, as was supposed from the literature references. Tubes of $BaMgTi_7O_{16}$ and rods of $K_2MgTi_7O_{16}$ were grown which were two-phase, polycrystalline, coarse grained orientated crystallites. It appears that a flux growth system could be used for both $BaMgTi_7O_{16}$ and $K_2MgTi_7O_{16}$ if solubility data is known.

Under an earlier NASA sponsored contract (NAS 3-14410), it was shown that sodium beta-alumina tubes could be grown by the EFG technique using iridium components. However, loss of sodium from the melt as a result of volatilization prevented the growth of stoichiometric single phase material. A primary goal of this present contract was therefore the design and construction of a furnace chamber which would allow the growth of crystals under inert gas pressures up to 2 MN/m^2.* By this method, we were able to suppress the loss of volatile constituents.

Single crystal, single phase tubes of beta-alumina containing Na_2O, $2Na_2O \cdot MgO$ and K_2O were grown as verified by Debye-Scherrer X-ray powder

*1 MN/m^2 = 145 psi.

patterns, Laue back reflection X-ray photographs, and chemical analysis. Only iridium components may be used without excessive erosion and dissolution of the crucible and the die material in the melt, and subsequent incorporation in the crystals grown.

The major problem to be solved is the tendency for the beta-alumina tube crystals to crack along the cleavage plane during growth, which is perpendicular to the c-axis and the slow growth speed required for successful growth. The use of an afterheater may be all that is required to solve both of these problems.

II. INTRODUCTION

There is a new group of materials which are of particular interest because of their potential use as ionic conductors and subsequent use as single crystal membranes in solid-state battery applications. The hollandite and hexatitanate compounds are of this group and are represented by $BaMgTi_7O_{16}$, $K_2MgTi_7O_{16}$, $K_{1.6}Mg_{0.8}Ti_{7.2}O_{16}$ (hollandite), and $Na_2Ti_6O_{13}$ (hexatitanate).[1-7]

Also in this group is beta-alumina which has been, for some time, in widespread use as a refractory material in the form of cast bricks. More recently, it has been proposed that it may have important future application as a membrane for high energy batteries. Ford Motor Company has demonstrated this potential with polycrystalline beta-alumina membranes and a liquid sodium-liquid sulphur system.[8,9]

The property of beta-alumina which allows it to be considered for this function is the anisotropy which its crystalline structure exhibits with respect to ionic conductivity, electronic conductivity being essentially negligible in all directions.[9-12] At room temperature, it is virtually nonconducting along the c-axis of the hexagonal cell, yet has a specific resistance of only 30 ohm-cm at right angles to this direction, i.e., along the a-axis. Obvious advantages in efficiency compared with polycrystalline aggregates will accrue from the use of single crystalline membranes of the correct orientation. Even if the polycrystalline aggregates are of preferred orientation, the presence of grain boundaries provides additional problems, since intergranular processes may occur, resulting in failure of the conducting path. Also, it is possible that lower operating temperatures may result from the use of single crystal materials. Thus, the establishment of a method for the growth of single crystalline beta-alumina is of considerable interest.

The objective of the present program was to establish the feasibility of growing single crystal tubes of beta-alumina and the hollandite and hexatitanate materials by making use of a novel crystal growing technique developed by Tyco Laboratories, Inc.[13,14] The design and construction of a high pressure furnace chamber which

would allow the growth of crystals under inert gas pressures of up to 2 MN/m^2 was a primary goal of this contract. This was necessitated by the fact that under an earlier NASA-sponsored contract[15] it was established that 100% beta-alumina crystals could not be grown without preventing the loss of sodium from the melt as a result of volatilization. It was also thought that the high pressure growth chamber may also be required for the growth of the hollandite and hexatitanate compounds, where similar volatilization problems are expected.

The original program was modified after 12 months so as to grow rods of $K_2MgTi_7O_{16}$ instead of tubes and to grow tubes of $K_2O \cdot 11\,Al_2O_3$ (beta-alumina) instead of $Na_2Ti_6O_{13}$, since that was no longer of interest as a potential solid electrolyte.

This report describes experiments and results on the growth of single crystalline tubes of $BaMgTi_7O_{16}$, $K_2MgTi_7O_{16}$, and beta-alumina.

III. APPARATUS AND BASIC EXPERIMENTAL PROCEDURES

The design and construction of a furnace chamber which would allow the growth of crystal under inert gas pressures up to 2 MN/m^2 (300 psi) was a primary goal of this contract. This was necessitated by the fact that single phase beta-alumina tubes could not be grown from the melt[15] because of the high loss of sodium by volitilization at the growth temperature under atmospheric conditions. It was found that the high pressure furnace was also required for the growth of the hollandite compounds ($K_2MgTi_7O_{16}$ and $K_{1.6}Mg_{0.8}Ti_{7.2}O_{16}$).

The high pressure furnace is shown schematically in Fig. 1 and was used for the growth of all beta-alumina tube crystals. The pressure vessel consists of a 30 cm diameter by approximately 60 cm high 304 S/S split chamber, designed for 2 MN/cm^2 at 541 K. The chamber is water jacketed and mounted on a suitable stand with a hand-operated hydraulic mechanism to raise and lower the bottom section approximately 30 cm. The lower section swings away in the lowered position for accessibility.

The furnace was designed to allow the growth of crystal tubes up to 20 cm long. and includes the following features:

1. On top is mounted a linear motion device suitable for withdrawal of crystals at rates of up to 2.5 cm/min.*

2. 10 cm port for RF power feedthroughs.

3. 5 cm inner dia sight ports (2) at 20° incline from horizontal.

4. 2.5 cm vacuum port.

5. Feedthroughs complete with manually-controlled x-y and verticle motion device allowing precise location of crucible (x-y motion is ± 6 mm and the vertical motion ± 13 mm).

---

*A.D. Little Co., Cambridge, Massachusetts

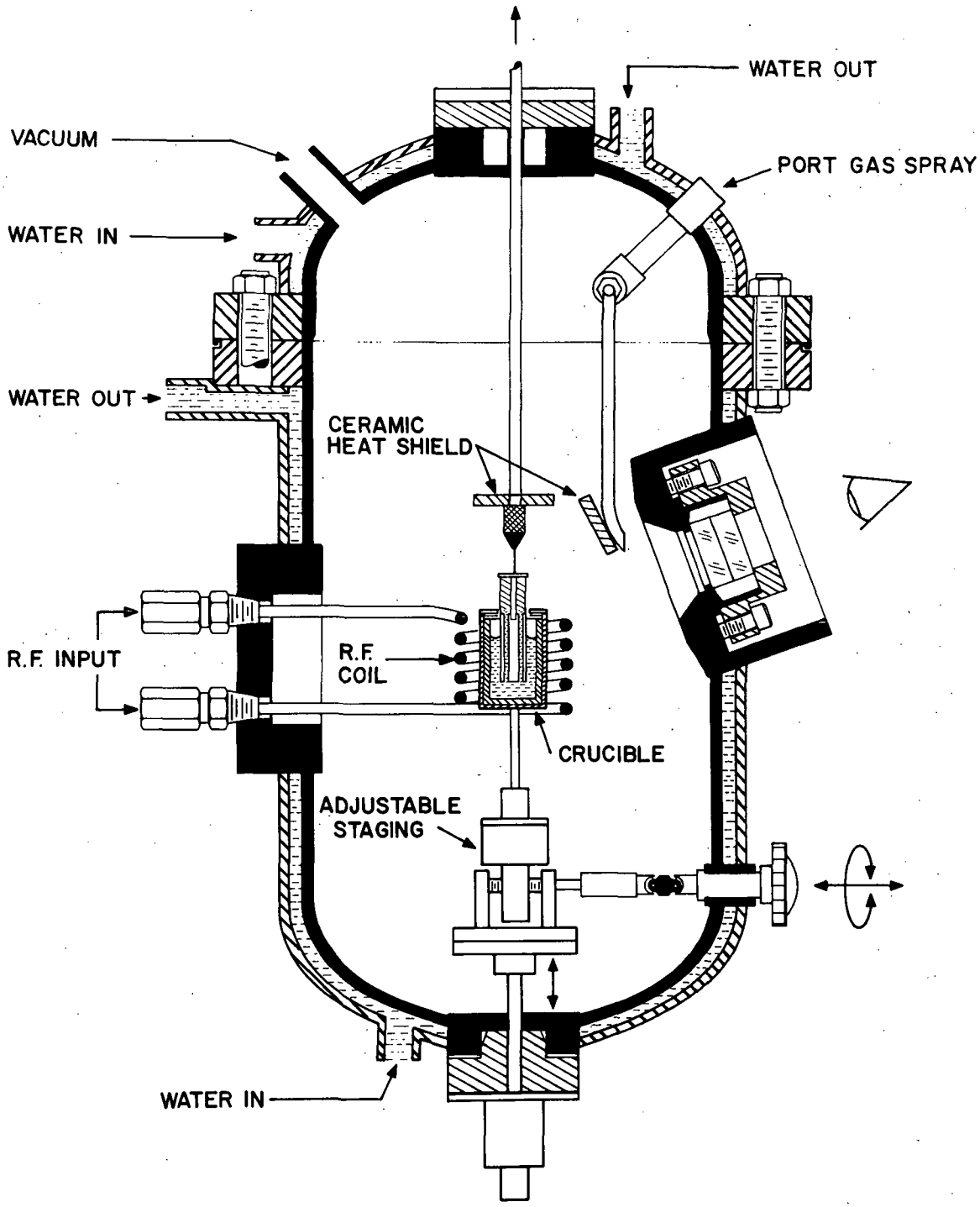

Fig. 1. Schematic of high pressure crystal growth chamber

6. Various 1.3 to 2.5 cm ports required for evacuation; introduction of inert gas and measurement of gas pressure.

The entire high pressure crystal growing furnace is shown photographed in Fig. 2.

An atmospheric pressure[16] furnace shown schematically in Fig. 3 was used for the growth of $BaMgTi_7O_1$ tubes and the initial growth of $K_2MgTi_7O_{16}$. An atmosphere, oxygen or argon in the present case, is maintained within the furnace, which consists of two concentric quartz tubes between which cooling water flows. The melt and growth area is viewed directly through either of the ports which allow essentially undistorted observation. The windowports are provided with a cover of optical quality glass. The inert gas flow (2) acts to prevent oxide deposition on the inside of the window and thus maintains clean observation conditions. The two ports are separated by 120° of arc. They allow both temperature measurements and control and optical monitoring of the growth procedures. They are at angles of 90° and 60° to the furnace axis in order to provide additional observation freedom of the area of interest. The overall system, including furnace, stereomicroscope viewer, pulling system, etc., is shown photographed in Fig. 4.

The pulling mechanism may be simply considered as two rigid parallel vertical shafts, one of which is an air bearing connected to a plate with guide bearings on either side of the opposite shaft. Using compressed air, the system is essentially frictionless. A ball disk integrator and synchronous motor are used to move the shaft holding the seed crystal. The length of growth available is ~75 cm, and constant growth speeds in the range 0.00004 to 1.65 cm/min may be selected. In order to maintain a beneficial furnace atmosphere and to prevent backstreaming of air into the system via the pulling rod exit, an expandable bellows arrangement was used as shown in Fig. 4.

In both the above-mentioned furnace systems, a 450 kHz 20 kW induction unit is used to raise the crucible containing the melt to the necessary growth temperature either by susception directly to the crucible or a susceptor surrounding it. Schematic diagrams of the setups used for the growth of rods and tubes are presented in Fig. 5. Crucibles and dies were fabricated from iridium, platinum, and molybdenum and will be described in the following appropriate sections.

Fifty grams each of $BaMgTi_7O_{16}$ and $K_2MgTi_7O_{16}$ were synthesized by solid-state reaction according to the equations:

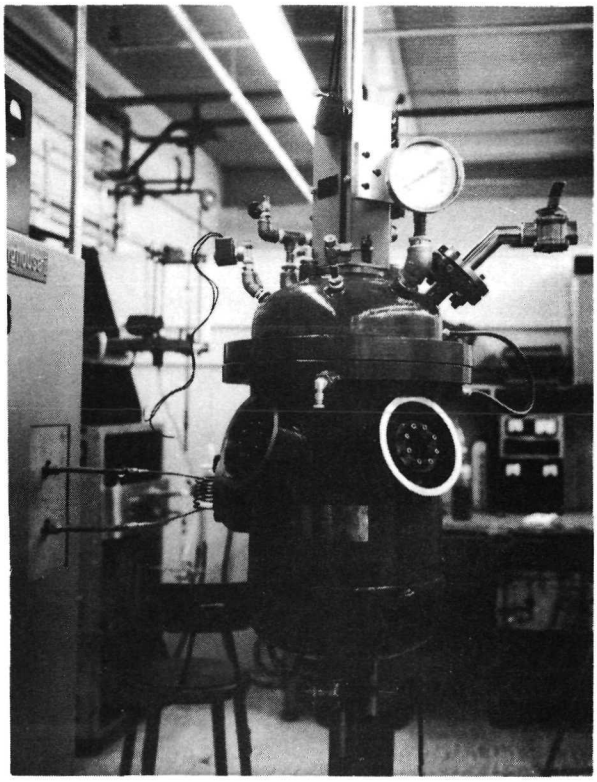

Fig. 2. High pressure crystal growth furnace

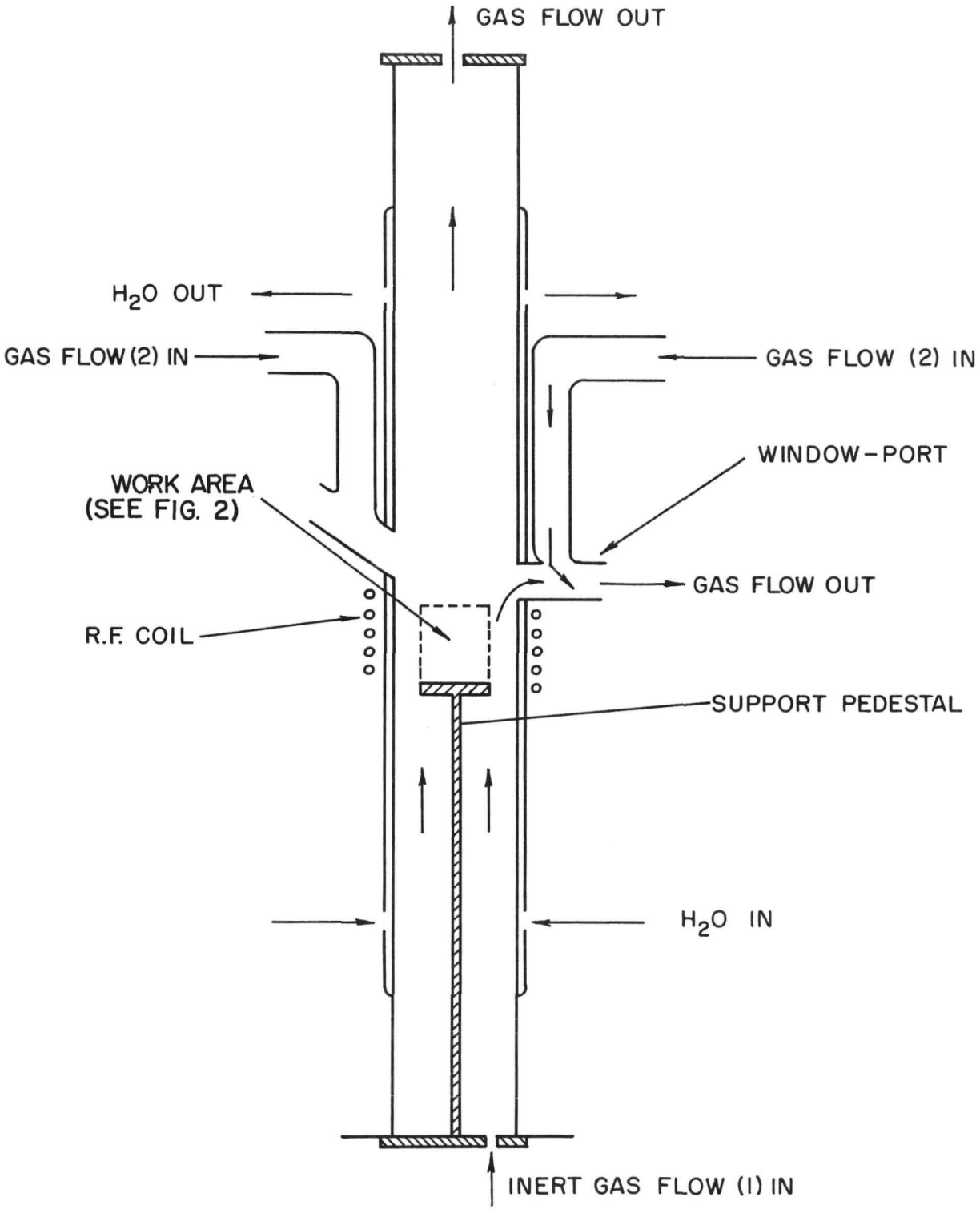

Fig. 3. Quartz furnace assembly incorporating two windowports

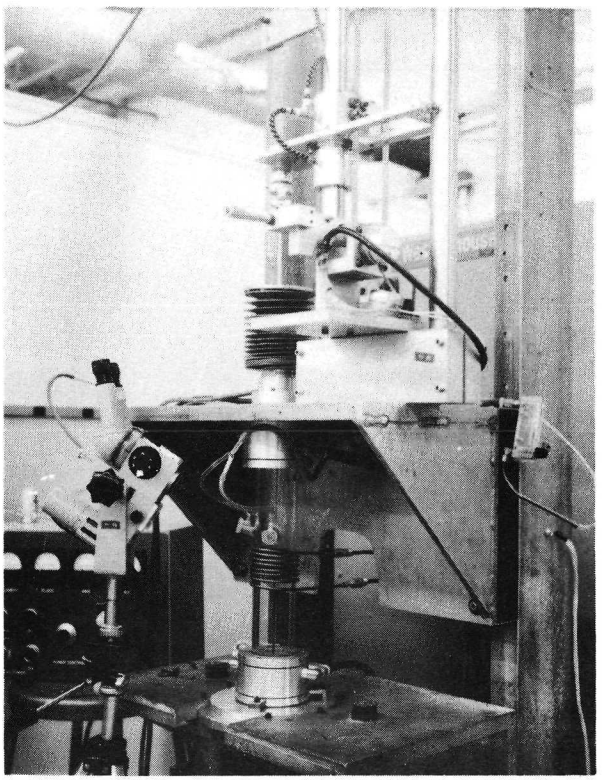

Fig. 4. Crystal growth apparatus

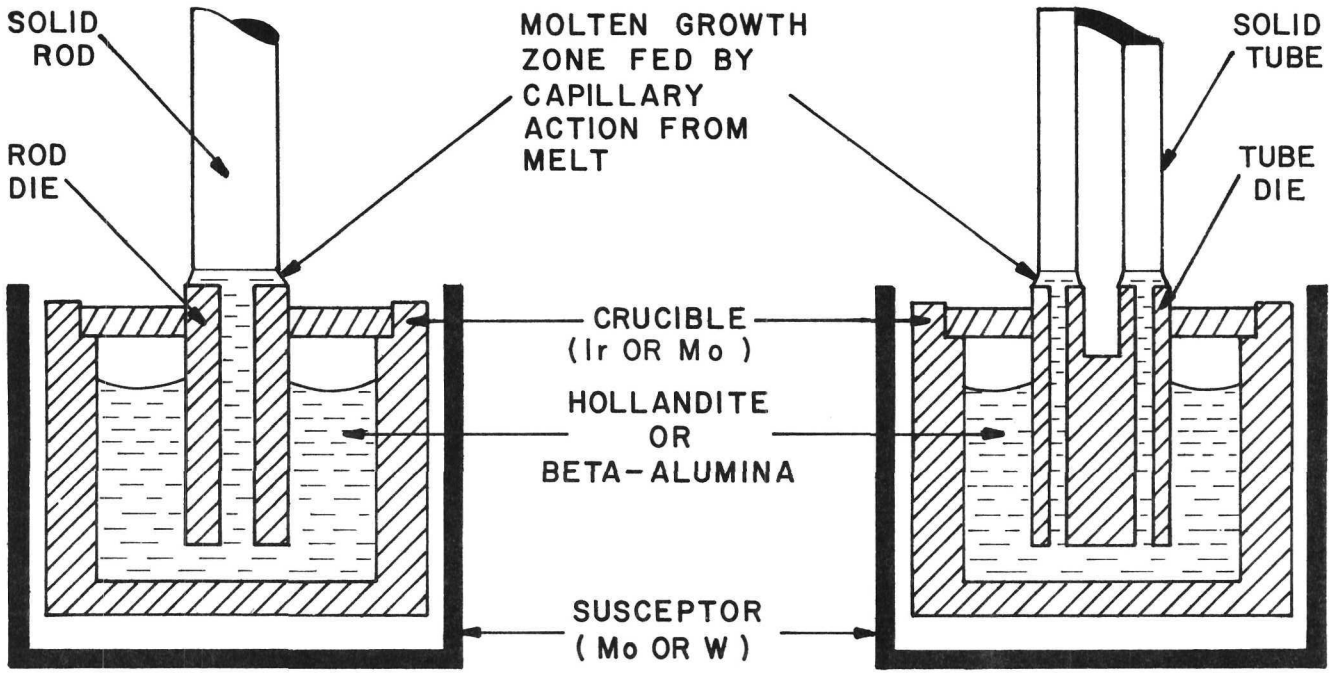

Fig. 5a. Schematic diagram showing crucible and die setup used for growth of rods

Fig. 5b. Schematic diagram showing crucible and die setup used for growth of tubes

$$BaCO_3 + MgO + 7TiO_2 \rightarrow BaMgTi_7O_{16} + CO_2$$

and

$$K_2CO_3 + MgO + 7TiO_2 \rightarrow K_2MgTi_7O_{16} + CO_2.$$

Stoichiometric proportions of the basic oxides and carbonates were thoroughly mixed and calcined at 1273 K for 15 to 20 h, in air, in platinum crucibles. The powders were then reground, pressed into 1.9 cm diameter pellets under a pressure of 20 MN/m^2, and refired at 1673 K ($BaMgTi_7O_{16}$) or 1423 K ($K_2MgTi_7O_{16}$) for 18 h in air. Debye-Scherrer (D/S) patterns were obtained from samples of each preparation lot. Hkl values, d-spacings, and line intensities for the first 30 or so recorded lines are presented in Tables I and II and compared with the literature values. Many more calculated lines than those previously reported as observed were noted. Some very weak lines attributed to unreacted TiO_2 ($BaMgTi_7O_{16}$), and partially reacted K_2TiO_{13} ($K_2MgTi_7O_{16}$) were also detected. It was expected that complete reaction, with no loss of components, would occur on melting, and no other premelting treatments were carried out.

Some preliminary wetting studies using $BaMgTi_7O_{16}$ and $K_2MgTi_7O_{16}$ (as prepared above) and small pieces of Ir, Pt - 20% Rh, and Pt were carried out. The molten material was observed to wet all three metal plates, without chemically reacting, and no problems were envisaged for the growth experiments.

There is a continuing uncertainty with regard to the exact composition of beta-alumina. The material commonly obtainable in such form and known as Carborundum Monofrax H beta-alumina is $Na_2O \cdot 11\ Al_2O_3$ (8.34 mole % Na_2O). This material was used for many of the growth experiments. Weber and Venero[17] reported the composition of beta-alumina as being 10 mole % Na_2O with a congruent melting point at (2240 ± 6) K. Mituo Harata[18] reported that Monofrax H cast bricks contain small amounts of alpha-alumina as a second phase and that there is a single phase area where beta-alumina exists. This area corresponds to Na_2O (10.9 to 13.7) mole % Na_2O. Monofrax H beta-alumina was used as the raw material in most beta-alumina growth experiments, with excess Na_2O added to vary the composition from 8.34% to 20% Na_2O. Calculated stoichiometric mixtures of Na_2CO_3 and Monofrax H beta-alumina were weighed into 5 to 11 g charges and placed in the iridium growth crucible and melted under 1.4 MN/m^2.

Table I. $BaMgTi_7O_{16}$ X-Ray Results CuK_α(Ni) 50 kV 20 mA

Standard Pattern[1,5]			Prepared Material		Grown Crystal	
$*I_{r(obs)}$[1]	$d_{(calc)}$[5]	$d_{(obs)}$[1]	I_r	d (Å)	I_r	d (Å)
vwd	7.149	7.12	vvw	7.1440	vvw	7.1530
w	5.055	5.06	w	5.0476	w	5.0248
w	3.574	3.55	sm	3.5719	m	3.5547
s	3.197	3.19	s	3.2456	w	3.2375
vwd	2.864	2.817	vs	3.1942	s	3.1921
—	2.528		wm	2.8413	vw	2.8399
ms	2.492	2.470	vwd	2.5680	vw	2.5460
—	2.383		sv	2.4820	ms	2.4780
vw	2.261	2.250	vwd	2.3041	mw	2.2539
m	2.235	2.223	mw	2.2542	m	2.2246
vwd	2.044	2.032	m	2.2249	vw	2.1885
vw	1.983	1.977	mw	2.1887	vw	2.0359
wm	1.895	1.884	vwd	2.0403	vw	1.9893
—	1.787		vvw	1.9668	vw	1.9629
—	1.734		m	1.8896	m	1.8861
m	1.685	1.683	sm	1.6861	m	1.6865
wm	1.599 1.589	1.583	w	1.1218	vw	1.6221
w	1.493	1.475	sm	1.5847	ms	1.5839
vw	1.461 1.452	1.446	wmd	1.4813	w	1.4817
—	1.429		w	1.4503	w	1.4517
vvw	1.432	1.415	vwd	1.4207	vw	1.4202
wm	1.402 1.396	1.390	md	1.3917	w	1.3958
—	1.378		wd	1.3737	w	1.3876
w	1.353 1.345	1.340	mw	1.3580	w	1.3576
vw	1.328	1.323	mw	1.3461	w	1.3457
w	1.114 1.111	1.113	vvw	1.3246	vw	1.3251
vw	1.033	1.026	vvw	1.1710	vw	1.1858
vw	1.011	1.007	vwd	1.1123	vw	1.1118
wd	0.8930	0.886	vw	1.0286	vw	1.0281
w	0.8794	0.873	vvw	1.0075	vw	0.9665
vw	0.8669	0.864	vw	0.8889	vw	0.8873
			vw	0.8763	w	0.8751
			vwd	0.8638	vw	0.8640

$*I_r$ = relative intensity
vs = very strong
s = strong
ms = medium strong
m = medium
w = weak
vw = very weak, etc.
d = diffused

Table II. $K_2MgTi_7O_{16}$ X-Ray Results CuK_α(Ni) 50 kV 20 mA

Standard Pattern[6]		Prepared Material		Grown Crystal		Powder from Furnace	
*I_r	d (Å)	I_r	d (Å)	I_r	d (Å)	I_r	d (Å)
		sb	7.7882	w	7.3627	vs	6.95
m	7.16	m	7.1598	sm	7.0418	w	3.745
m	5.08	wm	6.4337	wm	5.1642	s	3.47
		sm	5.0770	ms	5.0192	wm	3.145
w	3.592	vvw	4.4906	wm	3.5603	vw	3.028
		vvw	4.1965	w	3.4716	vw	2.905
		mw	3.6891	wm	3.2422	s	2.675
vs	3.211	mw	3.5865	vs	3.1854	sm	2.6035
		vs	3.2059	vvw	3.0675	w	2.389
		wm	3.0867	vw	2.7377	vw	2.321
w	2.538	wm	3.0451	m	2.5211	mw	2.259
s	2.487	md	2.9708	sv	2.4741	w	2.232
w	2.391	mw	2.7898	vvw	2.3769	w	1.997
w	2.271	mw	2.6958	sm	2.2593	wm	1.870
ms	2.235	w	2.5331	sv	2.2220	vvw	1.817
vvw	2.045	sm	2.4856	vvw	2.0381	w	1.742
w	1.991	mw	2.3746	m	1.9819	vw	1.646
ms	1.896	w	2.2626	sv	1.8897	sm	1.554
		m	2.2331	vw	1.8643	ms	1.517
		w	2.0991	vw	1.8396	wm	1.418
vw	1.794	w	2.0739	w	1.7857	vw	1.345
vw	1.740	vvwd	2.0384	w	1.7338	vw	1.340
m	1.691	vw	1.9895	ms	1.6865	vvw	1.3025
w	1.676	sm	1.8973	w	1.6698	vw	1.285
ms	1.592	vvw	1.7939	vs	1.5866	vvw	1.224
m	1.487	vw	1.7538	mw	1.4830	vvw	1.196
vw	1.457	vvw	1.7368	w	1.4509	vvw	1.1585
		m	1.6907	vw	1.4320	vvw	1.095
vw	1.426	vwd	1.6624	vw	1.4252	wm	1.0135
m	1.399	sm	1.5899	s	1.3952	vvw	0.996
w	1.349	mw	1.4868	wm	1.3467	vvw	0.987
vw	1.333	vwd	1.4545	mw	1.3285	vvw	0.960
vw	1.283	vwd	1.4257	w	1.2805	vvw	0.946
vw	1.263	m	1.3955	w	1.2602	w	0.896
		vw	1.3496	vw	1.2413	w	0.889
vw	1.196	vw	1.3313	mw	1.1940	vw	0.867
		vw	1.2806				
		vw	1.2609				
		mwd	1.1921				

*I_r = relative intensity
vs = very strong
s = strong
ms = medium strong
m = medium
w = weak
vw = very weak, etc.
d = diffused
b = broad

Rods and tubes were grown from hollandite and beta-alumina melts using the Tyco-developed melt growth technique, "edge-defined, film-fed growth" (EFG).[13,14] This technique is a modified melt-growth method which is akin to the old Czrochrolski method of crystal pulling and allows the growth of single crystals with constant, but almost arbitrary, cross-sectional shapes. The crystals grown were examined using optical microscopy in transmitted and reflected light. The composition and occurrence of second phase in the crystals grown was determined using standard Debye-Scherrer examination of powdered samples and comparing the pattern and line intensities with standard films (in the case of beta-alumina) and literature values (in the case of the hollandite compounds). Laue X-ray back reflection photography was used to study the crystallinity of the samples grown. An annealed piece of $BaMgTi_7O_{16}$ was analyzed by nondispersive X-ray spectroscopy using a scanning electron microscope (Fig. 6).

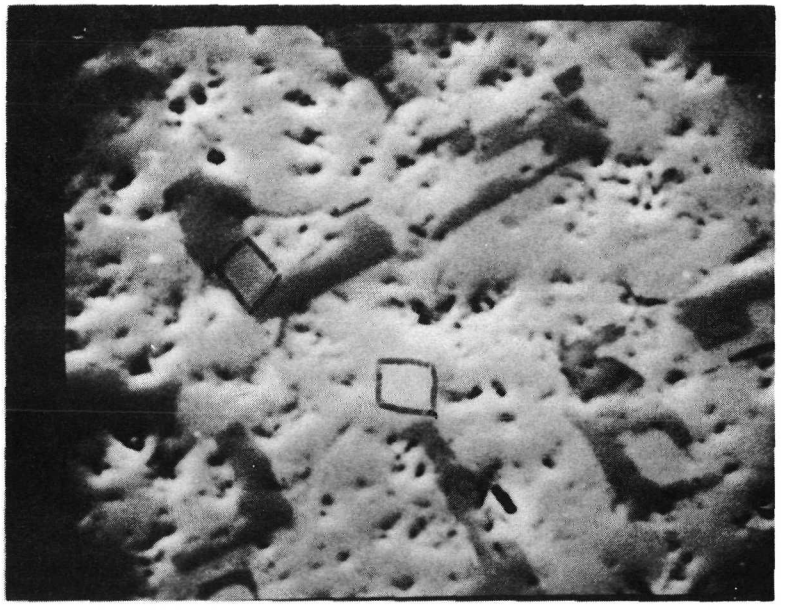

Fig. 6. Transverse section of $BaMgTi_7O_{16}$ tube No. 1 annealed for ~60 hr in air - O_2 (1000X); area inside the squares on matrix and angle bars is area analyzed by scanning electron microscope

IV. CRYSTAL GROWTH EXPERIMENTS

A. Hollandite - $BaMgTi_7O_{16}$

A crystal growth apparatus capable of growing $BaMgTi_7O_{16}$ tubes was assembled from iridium components. The die used allowed the growth of tubes 5 mm outer dia × 3.5 mm inner dia. All $BaMgTi_7O_{16}$ growth experiments were made using this iridium tube setup. Five of the growth experiments resulted in the formation of $BaMgTi_7O_{16}$ tubes.

All the growth experiments were made in air or O_2, inside a water cooled quartz tube, using a 20 kW, 450 KHz RF set as the power supply. (See Figs. 3 and 4). The 19 mm outer dia × 19 mm high × 0.5 mm wall iridium curcible, containing the calcined $BaMgTi_7O_{16}$ charge material, and the iridium tube die were both suscepted to directly. Manual temperature was achieved by a multiturn potentiometer arrangement of the RF manufacturers design.

The iridium crucible was raised to the melting point of the $BaMgTi_7O_{16}$ compound. When melting occurred, liquid charge material was seen to rise to the top surface of the tube die. Crystal growth was then nucleated on the end of a 1/4 mm dia iridium wire. During the initial growth experiments, some difficulty was encountered in causing the crystal to become a complete tube. This was overcome by increasing the temperature gradient and pulling speed. The growth experiments were performed at 5 to 11 cm/h. The tubes of $BaMgTi_7O_{16}$ consisted of coarse-grained orientated crystallites and were two-phased (~95% $BaMgTi_7O_{16}$ - 5% TiO_2), as determined by Debye-Scherrer powder patterns and metallography. (Table I and Fig. 6.) After growth, these crystals were bluish-black in color. As reported previously,[1] annealing at elevated temperatures (1073-1473 K) in air or oxygen changed the specimen color (to cream-yellow), but with no accompanying measurable gain in weight. Fig. 7 shows the typical appearance of unannealed and annealed tubes. Similar color changes have long been known in barium titanate

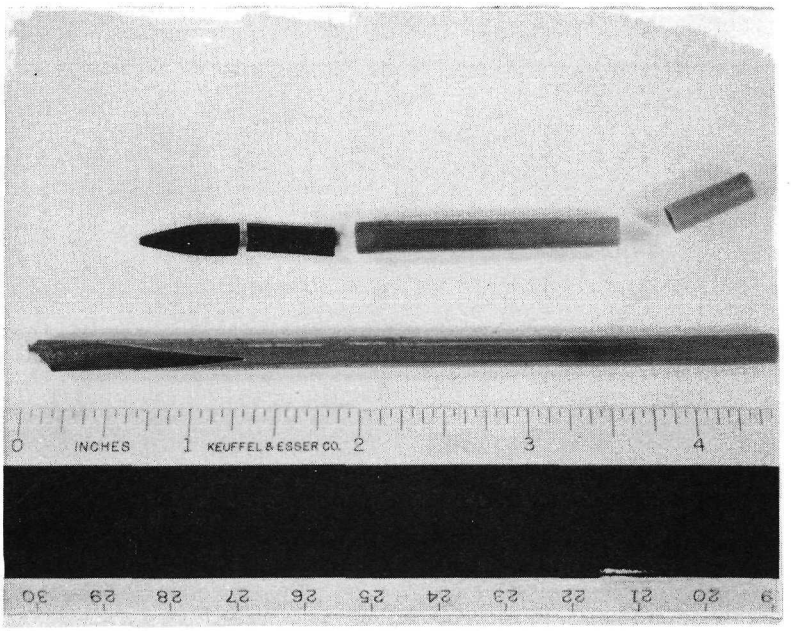

Fig. 7. Top row shows pieces of unannealed (bluish-black) and annealed (light yellow-brown) $BaMgTi_7O_{16}$ tube No. 1 (annealing was carried out for 90 h in flowing O_2 at 1323 K); the bottom row shows the $BaMgTi_7O_{16}$ tube No. 2 (annealed for 125 h in flowing O_2 at 1323 K)

compounds and are associated with the oxidation of titanium from Ti^{+3} to Ti^{+4}, the bluish-black color being due to oxygen deficiency. It should be noted that the $MgO-BaO-TiO_2$ section in the quaternary Mg-Ba-Ti-O system is, of course, not one of constant oxygen concentration.

The Debye-Scherrer patterns obtained from crushed samples of these tubes agree closely with that reported by Norrish,[5] using d values calculated using the lattice constants, a = 10.110 Å and c = 2.986 Å, reported by Dryden and Wadsley.[1] In addition, extra lines were found and identified as arising from the presence of rutile as a second phase. (See Table I.)

Wet chemical analysis of the overall tube composition is shown in Table III, together with the weight percent of each element present in the starting material. The apparent increase in Mg content may be due to the greater relative loss of Ba, Ti, and O during growth, since the melting point of BaO is only 2196 K and the decomposition temperature of TiO_2 is only 1913 K, while the melting point of MgO is 3073 K. The temperature of the melt was observed to be approximately 2023 K by optical pyrometry.

Table III. Nominal and Analyzed Tube Composition

	Calculated Wt % for $BaMgTi_7O_{16}$	Chemical Analysis Average Wt % (Both Tubes)	
		Tube No. 1	Tube No. 2
Ba	18.2403	18.1	17.95
Mg	3.2286	3.86	3.71
Ti	44.5315	45.2	45.1
O	33.9996	*32.84	*33.24

*Based on total content of Ba, Mg, and Ti.

An attempt at determining the orientation of the as-grown tubes No. 1 and No. 2 of $BaMgTi_7O_{16}$ was carried out using Laue back-reflection X-ray photographs. Great difficulty was encountered during our attempts to orientate the crystal due to fluorescence from the crystal. This caused the film to be over exposed in the center and identification of the exact growth direction impossible using this method. The principal determination that could be made from the Laue X-ray photographs was that the tubes appeared to be essentially single crystalline, even though they were two-phased microscopically. This was because the second phase (TiO_2) was oriented with respect to the $BaMg\ Ti_7O_{16}$ (hollandite) in the grown tubes. An annealed piece of tube No. 1 was analyzed by nondispersive X-rays using a scanning electron microscope. Figs. 6, 8, and 9 show a transverse section of this tube. As can be seen from these microphotographs, the tube consists of two major phases: a matrix phase and a phase which looks like angle bars. Nondispersive X-ray analysis of the indicated region in Fig. 6 shows the matrix to contain Ba, Mg, and Ti, while the angle bars contain Ti but not Ba or Mg. The scanning electron microscope was not capable of detecting oxygen. These results confirm the conclusions derived from the Debye-Scherrer X-ray powder patterns of as-grown and annealed samples of $BaMgTi_7O_{16}$ tube No. 1.

A Laue X-ray photograph of an annealed piece of tube No. 1 showed more distinct spots than the as-grown tube. From the Laue X-ray photographs taken of $BaMgTi_7O_{16}$ tubes No. 1 and No. 2, it appears that they were grown in the same direction, despite the fact that tube No. 2 was seeded by a piece of tube No. 1 which was orientated 90° from its growth direction. The common growth direction was determined to be along the c-axis of each grain by the observed cleavage as well as by optical extinction observations. Longitudinal and transverse sections were viewed under reflected polarized light. Since $BaMgTi_7O_{16}$ is tetragonal, an extinction position is observed upon rotation in polarized light about any axis not parallel to the c-axis. When viewed parallel to the c-axis, no extinction occurs. The extinction pattern of longitudinal and transverse sections showed that the tubes were grown parallel to the c-axis.

There is some evidence to indicate that the compound $BaMgTi_7O_{16}$ may not melt congruently. Fig. 9 shows a third phase which evidently was not detected by X-rays.

A growth experiment was performed from a melt containing 5 mole % excess Ba and 5 mole % excess Mg to try to reduce the amount of TiO_2 in the grown tube. The

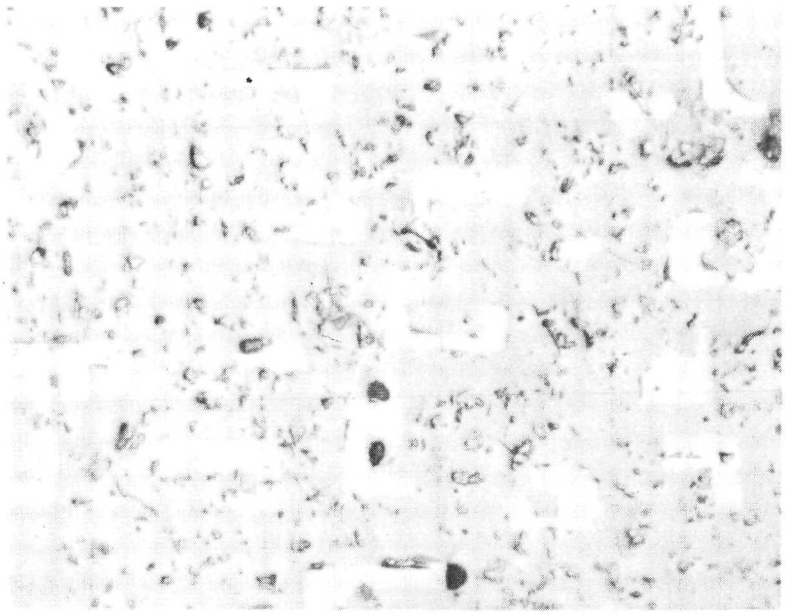

Fig. 8. $BaMgTi_7O_{16}$ tube transverse section, annealed; 60 h, 1323 K reflected light (750X)

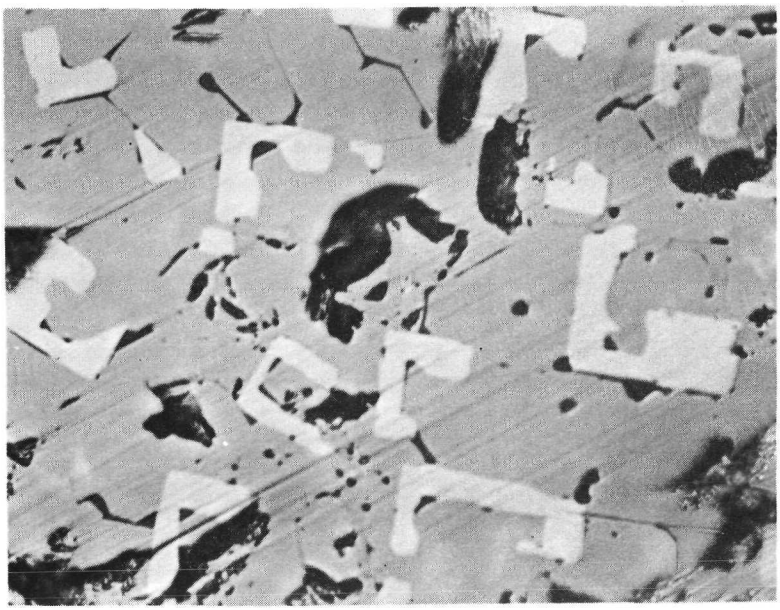

Fig. 9. $BaMgTi_7O_{16}$ tube transverse section, as-grown, reflected light (750X)

pattern obtained from this $Ba_{1.05}Mg_{1.05}Ti_7O_{16.1}$ tube was essentially the same as that obtained from tubes grown from the original composition $BaMgTi_7O_{16}$. The pattern indexed to $BaMgTi_7O_{16}$ (hollandite) and TiO_2 (rutile) in the ratio of ~95% to ~5%. We conclude, based on the abovementioned results, that growth in this system will not be possible until the phase diagram of this system is examined.

B. $K_2MgTi_7O_{16}$ - Hollandite

The initial tube growth experiments of $K_2MgTi_7O_{16}$ were performed using the same furnace, iridium setup, and procedure as that mentioned above for $BaMgTi_7O_{16}$. During the attempted growth experiments, the melt was observed to vary its melting point. As growth progressed at 3.8 cm/h, the melt at the top of the die would freeze and when remelted was observed to freeze at a higher temperature than before. Bubbling was also observed in the melt at the top of the iridium tube die. Because of these difficulties, it was not possible to grow a complete tube from the $K_2MgTi_7O_{16}$ melt. The growth experiments resulted in pieces of $K_2MgTi_7O_{16}$ which were not complete tubes. The color of the as-grown crystals varied from a bluish-black to a light brown. A piece of a crystal was examined using a Debye-Scherrer X-ray camera to see if the compound $K_2MgTi_7O_{16}$ was actually grown from the melt of the composition $K_2MgTi_7O_{16}$. There was also some volatilization associated with the atmospheric growth of $K_2MgTi_7O_{16}$ which resulted in a deposit being formed on the walls of the growth chamber. This powder was also examined using Debye-Scherrer X-ray techniques to see if it could be identified. The results listed in Table II show the standard pattern[1] for $K_2MgTi_7O_{16}$ compared to the starting material, the as-grown piece of $K_2MgTi_7O_{16}$, and the powder deposited in the growth chamber. From these results, it can be seen that the piece of as-grown crystal shows $K_2MgTi_7O_{16}$ with a slightly smaller lattice parameter and a few unidentified lines. The shift in the lattice parameter is probably due to the loss of one of the constituents in the compound. The powder pattern obtained for the deposited material in the growth chamber and listed in Table II was not identifiable. It does not appear to be a potassium oxide, titanate, or magnesium titanate.

Based on the above results, it was concluded that the high pressure furnace should be used in an attempt at producing $K_2MgTi_7O_{16}$ tubes or rods. Experiments were conducted under 0.7 to 1.4 MN/m^2 argon overpressure, and growth speeds varied from 2.5 to 65 cm/h. Pressures as low as 0.7 MN/m^2 appear to be effective in suppressing potassium vaporization. Melts were contained in both iridium and molybdenum crucibles, and both iridium and molybdenum were used as die components. Growth was nucleated on the end of a 1/4 mm dia platinum or molybdenum wire.

Several growth experiments were performed in an attempt at producing $K_2MgTi_7O_{16}$ tubes. During all growth attempts, the crystals could not be encouraged to spread into a complete tube. As was the case of the growth experiments performed at atmospheric pressure while growth was taking place, there was liquid and solid at the melt interface at the same time. A sample composed of coarse-grained orientated crystallites 19 mm long with a 6 mm circle radius was the best result.

Because of the difficulty encountered in trying to produce $K_2MgTi_7O_{16}$ tubes, it was decided to attempt to grow $K_2MgTi_7O_{16}$ rods from either iridium, platinum or molybdenum setups. Some success was encountered in growing a polycrystalline rod 6 mm in dia and 10 mm long from an iridium rod die. Molybdenum components were used for the growth of 3 mm dia $K_2MgTi_7O_{16}$ rods. Even though rods were able to be produced, there was always the appearance of liquid and solid at the melt interface. The as-grown color of the $K_2MgTi_7O_{16}$ rods was a bluish-black, which became a cream color upon annealing in air at ~1273 K for 15 h. All of the above-mentioned crystals were composed of coarse-grained orientated crystallites which appeared orientated so that the long axis (c-axis) was parallel to the growth direction. This is 90° from the desired direction, which is with the c-axis perpendicular to the growth axis.

Samples of the $K_2MgTi_7O_{16}$ rods grown from both iridium and molybdenum setups were examined using Debye-Scherrer X-ray techniques and metallography. As was the case of the $K_2MgTi_7O_{16}$ grown at atmospheric pressure, the X-ray pattern obtained consisted of ~90% $K_2MgTi_7O_{16}$ with a slightly smaller lattice and ~10% of an unidentified phase (Table II). The metallographic sample consisted of two phases in the as-grown and annealed condition. Fig. 10 shows a transverse section of a 6 mm $K_2MgTi_7O_{16}$ as-grown rod. Based on the above-mentioned results, it can be concluded that single crystal growth will not be possible until the K_2O - MgO - TiO_2 system is more thoroughly investigated.

C. Sodium Beta-Alumina

There are considerable difficulties associated with the crystal growth of sodium beta-alumina. The difficulties are due principally to the fact that the compound appears to decompose peritectically[19] as well as due to the high vapor pressure of sodium over beta-alumina at its decomposition temperature.[9]

During the initial growth experiments, considerable difficulty was encountered with localized overheating of the Conax fittings and the power port to which they were

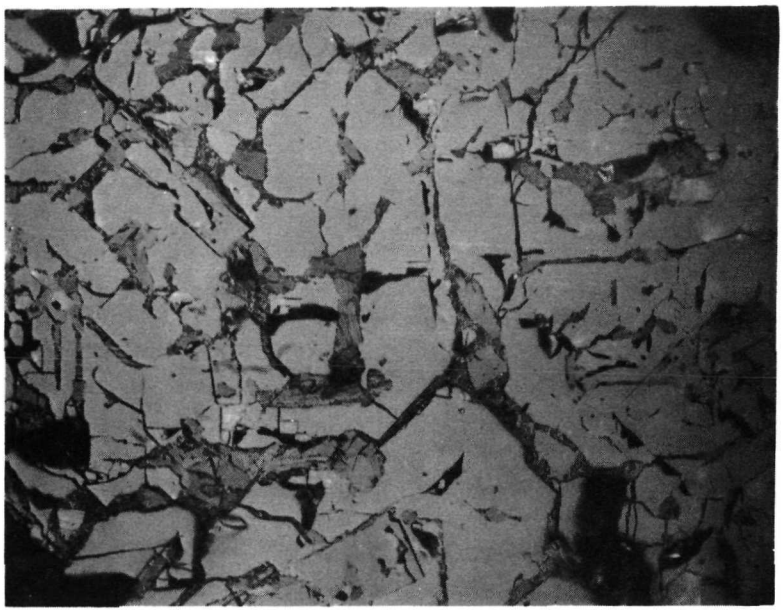

Fig. 10. $K_2MgTi_7O_{16}$ rod, as-grown from iridium setup (150 X); transverse section

connected. These problems were overcome by modifying the Conax fittings to accept fiberglass-reinforced Teflon pressure plugs and by water cooling the power port.

Difficulty was also encountered with arcing from the interior coil to any available groundpoint due to the presence of sodium vapor. This was initially prevented by coating the coil with a high dielectric constant film called "Durafilm 111 - Dielectric Enamel."* After several growth experiments using this coating, it was found to be sensitive to alkylides and was replaced with "Durafilm 300 Series"* dielectric enamel, which is insensitive to alkylides. In addition, the crucible, gas inlet tube, and seed holder have been electrically insulated from the pressure chamber with boron nitride inserts and ceramic shields. (See Fig. 1.)

In order to establish the amount of gas overpressure required for the growth of 100% beta-alumina, growth experiments were conducted at 0.7, 1.4, and 2 MN/m^2. All the growth experiments were conducted using iridium crucible and die components, with Monofrax H beta-alumina as the raw material and argon as the inert gas. Growth experiments were performed in the a-axis and c-axis directions at speeds of 1/4 to 5 cm/h. The seeds used to initiate growth were pieces of Monofrax H single crystals orientated in either the a or c-axis direction. The influence of inert gas overpressure is shown by Table IV, which gives the approximate relative beta-alumina and alpha-alumina composition of tubes grown under increasing inert gas overpressure. In each case, the starting melt composition had the approximate composition $Na_2O \cdot 11\ Al_2O_3$. As may be seen, there is a clear tendency for the relative percentage of beta-alumina present in the crystal tube to increase as the overpressure is increased from atmospheric to 1.4 MN/m^2. Beyond this, however, a further increase in pressure to 2 MN/m^2 does not give a further increase in beta-alumina content. This effect could be due to local convection currents[21] but is more likely associated with the incongruent melting of beta-alumina.[17,19] These beta alumina percentages were determined by comparison of the intensities of alpha-alumina and beta-alumina X-ray reflections as observed in Debye-Scherrer photographs as well as from metallographic observations. Although a single beta-alumina crystal was uses as seed in every case, none of the tubes where the beta-alumina content was not 100% was single crystalline. These results, together with data published by Metuo Harata,[18] in which he shows that Monofrax H cast bricks contain small amounts of alpha-alumina as a second phase, convinced us that growth of 100% beta-alumina would not be possible without the addition of excess Na_2O. To prepare tubes having a 100% beta-alumina composition as well as a substantial single

*American Durafilm Co., Inc., Newton Lower Falls, Massachusetts

Table IV. Alpha (Al_2O_3) and Beta-Alumina Contents of Tubes Grown under Inert Gas Overpressure (Compositions determined by Metallographic and Debye-Scherrer X-Ray Powder Pattern Measurements)

Starting Composition (mole % Na_2O)	Inert Gas Pressure (MN/m^2)	Percent Beta-Alumina	Growth Number
8.34	Atmospheric	40%	LP 8
8.34	0.7	75%	HP 4
8.34	1.4	85 to 90%	HP 9
8.34	2	85 to 90%	HP 10
20.0	1.4	100%	HP 15

crystallinity, it has been necessary to use melts containing an excess of Na_2O. As illustrated in Table IV for the case of tube No. H. P. 15, the use of a melt composition that contained an enriched Na_2O content enables tubes having a 100% beta-alumina content to be grown.

Often the as-grown tubes were covered with a grayish-white deposit. In most cases this was successfully removed by annealing the tubes at 1523 K, which is above the decomposition temperature of Na_2O. Cracking was also a problem that was encountered during growth and seemed to occur more at high growth rates ($>$ 6 mm/h) than at slow rates ($\sim$ 2 mm/h). The cracking always occurred in the cleavage plane, which is perpendicular to the c-axis. In one instance, a grown crystal that was uncracked and left to stand in the growth chamber for 72 h in room atmosphere was found wet and cracked in three places upon removal from the furnace.

A photograph of four beta-alumina tubes is shown in Fig. 11. Two of the four crystals are 100% beta-alumina: H. P. 11 a-axis growth and H. P. 15 c-axis growth. Fig. 12 is a Laue back-reflection photograph taken from the bottom of tube H. P. 15 beta-alumina and confirms that this tube is substantially single crystalline. It has taken up the orientation of the seed crystal that is with the high conductivity planes normal to the tube axis.

Table V lists the chemical composition for tube H. P. 15 beta-alumina grown from a melt of composition $(Na_2O)_{0.2}\ (Al_2O_3)_{0.8}$. As can be seen from the table, the tube contains more Na than is found in $Na_2O \cdot 11\ Al_2O_3$, yet still retains the beta-alumina structure, as determined by Debye-Scherrer powder patterns and Laue back-reflection X-ray photographs (Fig. 12).

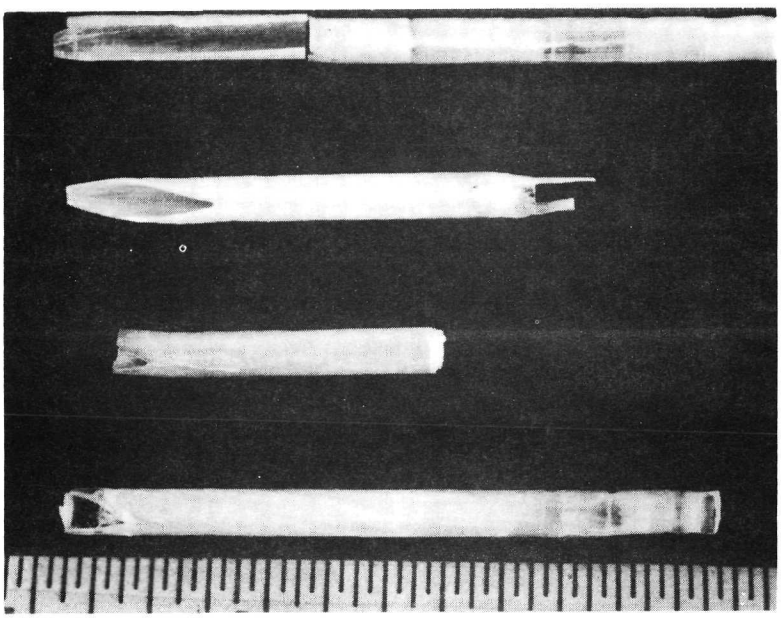

Fig. 11. Top to bottom H.P. 11 beta-alumina, H.P. 12 beta-alumina, H.P. 15 beta-alumina, and H.P. 17 beta-alumina, all annealed ~12 h at 1473 K in air

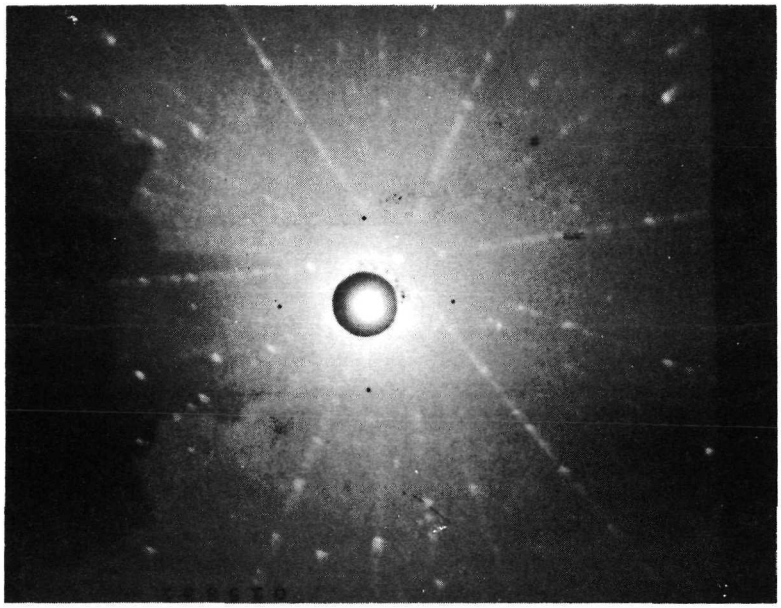

Fig. 12. Laue back-reflection X-ray photograph taken of bottom of beta-alumina tube H.P. 15 parallel to growth direction

Table V. Composition of Tube Crystals

Crystal		Analysis (Wt %)				Mole %		
		Na	Mg	Al	O	Na_2O	MgO	Al_2O_3
H. P. 15	Charge					20.0	–	80.0
	Top	6.8	–	63.6	(29.6)	11.1	–	88.8
	Bottom	7.5	–	56.3	(36.2)	13.5	–	86.6
H. P. 30	Charge					7.95	4.68	87.5
	Top	4.4	0.7	46.9	(48.0)	9.6	2.9	87.5
	Bottom	5.0	0.9	47.0	(47.1)	10.7	3.8	85.5

The use of an excess Na_2O melt composition together with a high inert gas overpressure is sufficient to overcome the problem associated with the high vapor pressure of sodium as well as with the possible incongruent melting of beta-alumina. The use of a 1:4 molar ratio of Na_2O to Al_2O_3, as the melt, constituents an essentially flux growth process which allows growth at ~50°C below that required for $Na_2O \cdot 11\ Al_2O_3$. These results show that properly orientated single crystal beta alumina tubes can be produced relatively crack-free, if the growth rate is 1/4 cm/h. The addition of an afterheater would have the twofold advantage of preventing deposits from forming on the tubes and preventing cracking.

D. Sodium Magnesium Beta-Alumina

The techniques and equipment used to grow beta-alumina plus magnesium oxide were the same as those mentioned above for the growth of sodium beta-alumina. Growth was performed in the c-axis direction using a piece of Monofrax H single crystal as a seed, and growth was performed under 1.4 to 1.7 MN/m^2 argon overpressure at pulling speeds from 2 to 6 mm/h. The starting material was 5 g of Monofrax H beta-alumina, to which was added 0.05 g excess Na_2O in the form of Na_2CO_3 and 0.1 g of MgO. This gave a starting composition of $\sim(2\ Na_2O \cdot MgO)_{0.14}$ $(Al_2O_3)_{0.86}$. Fig. 13 (a) and (b) shows two MgO doped beta-alumina tubes grown during these experiments. As can be seen from the Laue back-reflection photographs of crystal number H. P. 30, the crystal is essentially single crystalline, with the

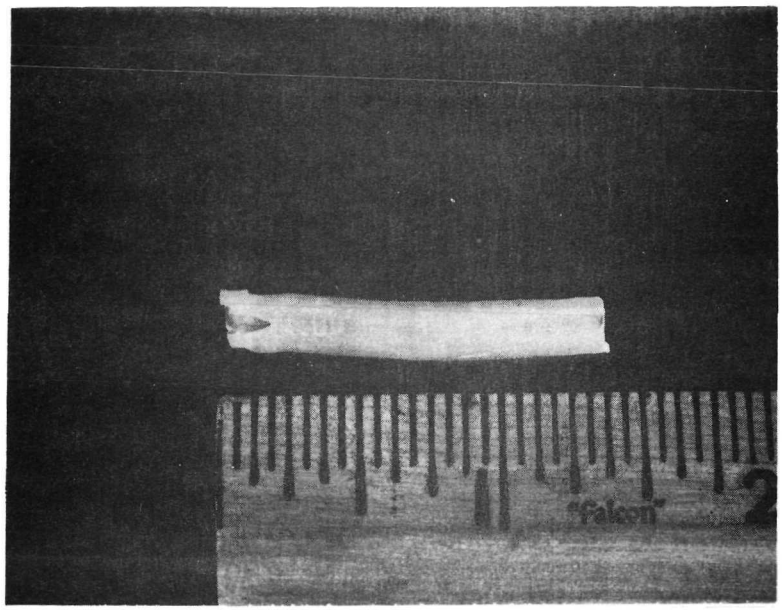

Fig. 13a. H.P. 30 beta-alumina plus magnesium oxide

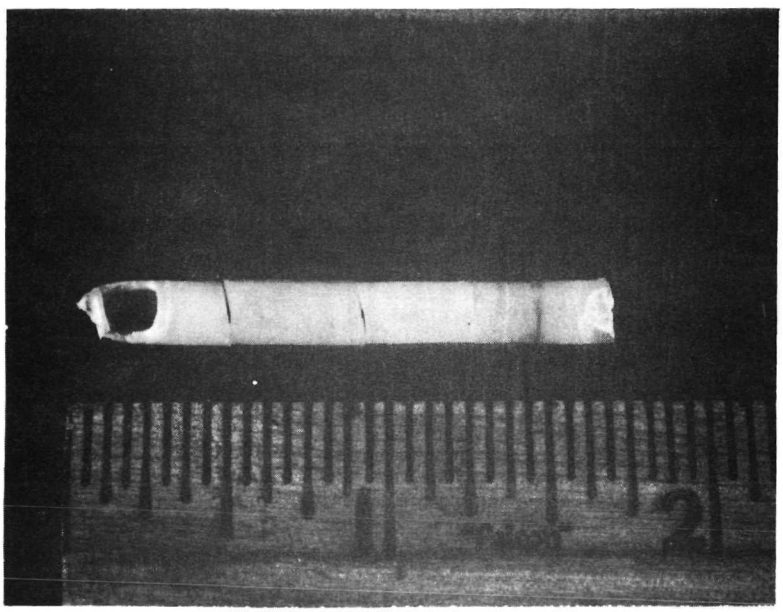

Fig. 13b. H.P. 31 beta-alumina plus magnesium oxide

c-axis parallel to the growth direction (Fig. 14). Table V list the chemical analysis for tube H. P. 30. The analysis shows the tube to contain less magnesium oxide than was in the starting material and cannot be explained at this time. Debye-Scherrer powder patterns taken of the tube show it to have the beta-alumina structure. It is concluded from these results that it is no more difficult to grow beta-alumina with magnesium oxide additions than undoped beta-alumina.

E. Potassium Beta-Alumina

One growth experiment on potassium beta-alumina was performed. The starting material for the growth experiment was potassium beta-alumina which was prepared by leaching sodium beta-alumina in KNO_3 (method supplied by NASA-Lewis). Analysis after the four leaching treatments showed that 98% of the sodium in Monofrax H had been exchanged by potassium. The seed was a c-axis oriented crystal of Monofrax H. Growth was performed in the high pressure crystal puller under 1.4 MN/m^2 argon overpressure at ~ 6mm/h. Upon initiating growth, the seed broke loose from the Al_2O_3 1/2 mm diameter filament it was attached to, so growth was then nucleated on the Al_2O_3 filament. Growth continued until the crystal froze to the tube die terminating the growth experiment. The resulting tube crystal had several cracks in it due to freezing problems during growth, but was 32 mm long and did not have a deposit on it from growth. Both cracking problems were due to a crack developing in the molybdenum susceptor. Observed cleavage showed the crystal was grown in the a-axis direction, and the Debye-Scherrer X-ray powder pattern showed it to be 100% potassium beta-alumina.

From the above mentioned results, it has been concluded that potassium beta-alumina is no more difficult to grow than sodium beta-alumina.

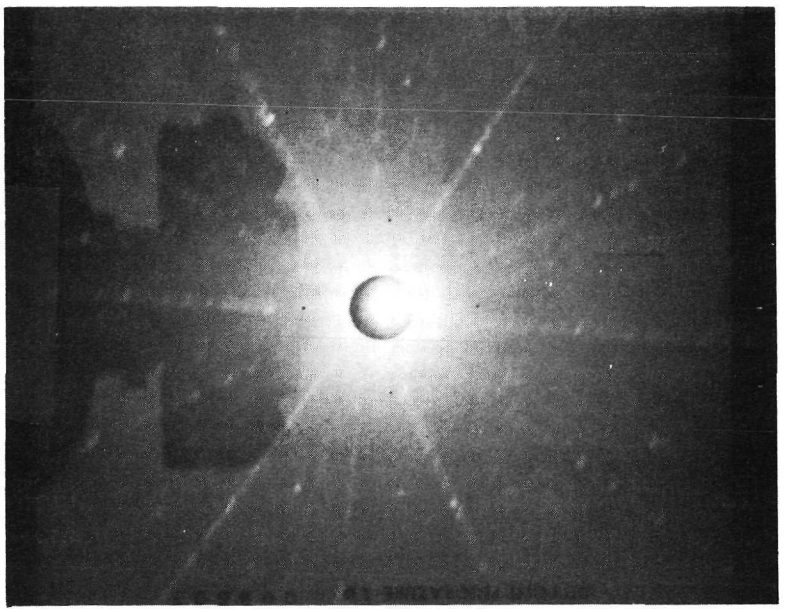

Fig. 14a. Laue of bottom of H.P. 30 beta-alumina plus magnesium oxide tube parallel to growth direction

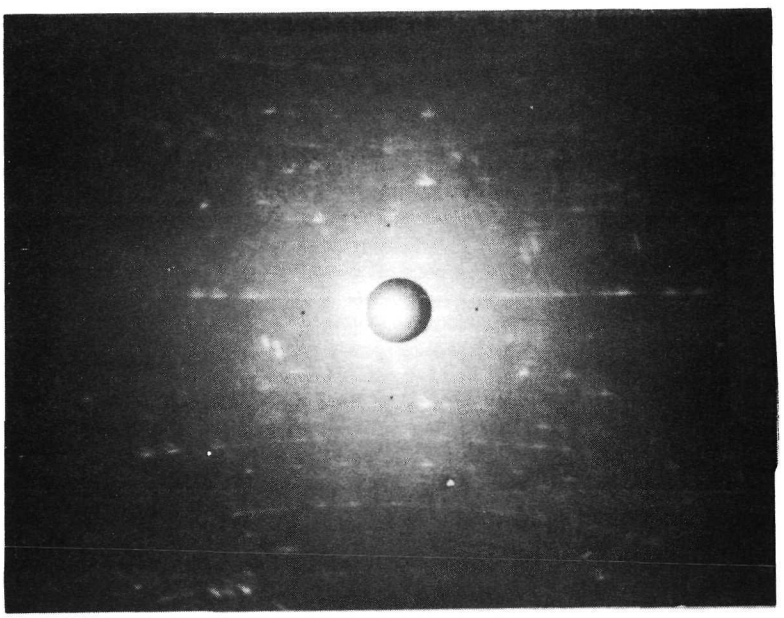

Fig. 14b. Laue of side of H.P. 30 beta-alumina plus magnesium oxide tube perpendicular to growth direction

V. CONCLUSIONS

Although tubes of $BaMgTi_7O_{16}$ and rods of $K_2MgTi_7O_{16}$ were grown, they consisted of coarse-grained orientated crystallites which were two-phase. It was concluded from these experiments that neither $BaMgTi_7O_{16}$ or $K_2MgTi_7O_{16}$ melt congruently, and therefore these compounds will be extremely difficult to grow by EFG until more phase diagram information is learned. Crystal growth from a flux system may be possible for both $BaMgTi_7O_{16}$ and $K_2MgTi_7O_{16}$, provided solubility data for these materials have first been obtained.

It has been demonstrated that melt growth of single crystal beta-alumina tubes using the EFG technique developed by Tyco Laboratories is feasible. The successful crystal growth of both beta-alumina and beta-alumina with magnesium oxide additions has been accomplished using the high pressure crystal puller designed and built during this contract. Laue back-reflection photographs, Debye-Scherrer powder patterns, and chemical analysis data all confirm the fact that 100% beta-alumina was grown, which was single crystalline and orientated in the c-axis direction.

Further work is necessary on increasing the growth rate, reducing the cracking, and preventing surface contamination during growth. The latter problems can probably be solved by the use of an afterheater.

VI. REFERENCES

1. I. S. Dryden and A. D. Wadsley, Trans. Far. Soc., 54, 1574-80 (1958).
2. S. Anderson and A. D. Wadsley, Acta. Cryst., 15, 194 (1962).
3. R. J. Gelsing, et al., Recueil, 84, 1452 (1965).
4. A. D. Wadsley in "Non-Stoichiometric Compounds," L. Mandelcorn (ed.), p. 99, Academic Press, N.Y. (1964).
5. K. Norrish, Min. Mag., 29, 496 (1951).
6. G. Bayer and W. Hoffman, Am. Mineral, 51, 511 (1966).
7. A. Bystrom and A. M. Bystrom, Acta. Cryst., 3, 146 (1950).
8. N. Weber and J. T. Krummer, Advances in Energy Conversion Engineering, 1967 Intersociety Energy Conversion Engineering Conference, p. 913.
9. J. T. Kummer, Progress in Solid State Chemistry, 7, (1972).
10. M. S. Wittingham and R. A. Huggins, J. of Chem. Phys., 54 (1971).
11. Yung-Fong Yee Sao and J. T. Kummer, J. Inog. Nucl. Chem., 29, 2453 (1967).
12. M. J. Rice and W. L. Roth, J. of Solid State Chem., 4, 294-310 (1972).
13. A. I. Mlavsky and H. E. LaBelle, Jr., Mat. Res. Bull., 6, 571 (1971).
14. H. E. LaBelle, Jr., Mat. Res. Bull., 6 581 (1971).
15. J. T. A. Pollock, R. Stormont, and F. Wald, Final Report, NASA Lewis Research Center, Contract NAS 3-14410.
16. H. E. LaBelle, Jr. and J. T. A. Pollock, Rev. of Sci. Inst., 42, 160 (1971).
17. N. Weber and A. F. Venero, Revision of the Phase Diagram $NaAlO_2$ - Al_2O_3, Annual Meeting of Americal Society, May 1970.
18. Mituo Harata, Mat. Res. Bull., Vol. 6, p. 461-464 (1971).
19. R. C. DeVries and W. L. Roth, J. of the Am. Ceram. Soc., 52, 364 (1969).
20. J. T. Kummer and Neil Weber, U.S. Patent No. 3, 413, 510, Nov. 26, 1968.
21. M. Chesswas, B. Cockayne, D. T. J. Hurle, E. Jakeman, and J. B. Mullin, J. of Crystal Growth, 11, 225-232 (1971).

DISTRIBUTION LIST

NASA

National Aeronautics and Space Administration
Scientific and Technical Information Facility
P. O. Box 33
College Park, MD 20740
(2 copies and 1 reproducible)

Mr. Ernst M. Cohn, Code RPP
National Aeronautics and Space Administration
Washington, DC 20546

Dr. A. M. Greg Andrus, Code SCC
National Aeronautics and Space Administration
Washington, DC 20546

Mr. Gerald Halpert, Code 764
Goddard Space Flight Center
National Aeronautics and Space Administration
Greenbelt, MD 20771

Mr. Thomas Hennigan, Code 761
Goddard Space Flight Center
National Aeronautics and Space Administration
Greenbelt, MD 20771

Mr. Louis Wilson, Code 450
Goddard Space Flight Center
National Aeronautics and Space Administration
Greenbelt, MD 20771

Mr. Jack E. Zanks, MS 488
Langley Research Center
National Aeronautics and Space Administration
Hampton, VA 23365

Dr. Louis Rosenblum, MS 302-1
Lewis Research Center
National Aeronautics and Space Administration
21000 Brookpark Road
Cleveland, OH 44135

Mr. Harvey Schwartz, MS 309-1
Lewis Research Center
National Aeronautics and Space Administration
21000 Brookpark Road
Cleveland, OH 44135

Dr. J. Stuart Fordyce, MS 309-1
Lewis Research Center
National Aeronautics and Space Administration
21000 Brookpark Road
Cleveland, OH 44135

Mr. Charles B. Graff, S&E-ASTR-EP
George C. Marshall Space Flight Center
National Aeronautics and Space Administration
Huntsville, AL 35812

Mr. W. E. Rice, EP5
Manned Spacecraft Center
National Aeronautics and Space Administration
Houston, TX 77058

JPL

Mr. Daniel Runkle, MS 198-220
Jet Propulsion Laboratory
4800 Oak Grove Drive
Pasadena, CA 91103

Mr. Aiji A. Uchiyama, MS 198-220
Jet Propulsion Laboratory
4800 Oak Grove Drive
Pasadena, CA 91103

Dr. R. Lutwack, MS 198-220
Jet Propulsion Laboratory
4800 Oak Grove Drive
Pasadena, CA 91103

ARMY

U. S. Army
Electro Technology Laboratory
Energy Conversion Research Division
MERDC
Fort Belvoir, VA 22060

Distribution List (Cont.)

ARMY (Cont)

Harry Diamond Laboratories
Room 300, Building 92
Connecticut Ave & Van Ness St., N.W.
Washington, DC 20438

U. S. Army Electronics Command
Attn: AMSEL-TL-P
Fort Monmouth, NJ 07703

NAVY

Director, Power Program, Code 473
Office of Naval Research
Arlington, VA 22217

Mr. Harry W. Fox, Code 472
Office of Naval Research
Arlington, VA 22217

Mr. S. Schuldiner, Code 6160
Naval Research Laboratory
4555 Overlook Avenue, S.W.
Washington, DC 20360

Mr. J. H. Harrison, Code A731
Naval Ship R&D Laboratory
Annapolis, MD 21402

Commanding Officer
Naval Ammunition Depot
(305, Mr. D. G. Miley)
Crane, Indiana 47522

Chemical Laboratory, Code 134.1
Mare Island Naval Shipyard
Vallejo, CA 94592

Mr. Phillip B. Cole, Code 232
Naval Ordnance Laboratory
Silver Spring, MD 20910

Mr. Albert Himy, 6157D
Naval Ship Engineering Center
Center Bldg., Prince Georges Center
Hyattsville, MD 20782

Mr. Robert E. Trumbule, STIC
4301 Suitland Road
Suitland, MD 20390

Mr. Bernard B. Rosenbaum, Code 03422
Naval Ship Systems Command
Washington, DC 20360

AIR FORCE

Mr. R. L. Kerr, POE-1
AF Aero Propulsion Laboratory
Wright-Patterson AFB, OH 45433

Mr. Edward Raskind, LCC, Wing F
AF Cambridge Research Laboratory
L. G. Hanscom Field
Bedford, MA 01731

Mr. Frank J. Mollura, TSGD
Rome Air Development Center
Griffiss AFB, NY 13440

HQ SAMSO (SMTAE/Lt. R. Ballard)
Los Angeles Air Force Station
Los Angeles, CA 90045

OTHER GOVERNMENT ORGANIZATIONS

Dr. Jesse C. Denton
National Science Foundation
1800 G Street, N.W.
Washington, DC 20550

PRIVATE ORGANIZATIONS

Aerospace Corporation
Attn: Library Acquisition Group
P. O. Box 95085
Los Angeles, CA 90045

Dr. R. T. Foley
Chemistry Department
American University
Massachusetts and Nebraska Avenues, N.W.
Washington, DC 20016

Dr. H. L. Recht
Atomics International Division
North American Aviation, Inc.
P. O. Box 309
Canoga Park, CA 91304

Mr. R. F. Fogle, GF 18
Autonetics Division, NAR
P. O. Box 4181
Anaheim, CA 92803

Dr. John McCallum
Battelle Memorial Institute
505 King Avenue
Columbus, OH 43201

Distribution List (Cont.)

Mr. W. W. Hough
Bellcomm, Inc.
955 L'Enfant Plaza, S.W.
Washington, DC 20024

Mr. D. O. Feder
Bell Telephone Laboratories, Inc.
Murray Hill, NJ 07974

Dr. Carl Berger
13401 Kootenay Drive
Santa Ana, CA 92705

Mr. Sidney Gross
M. S. 84-79
The Boeing Company
P. O. Box 3999
Seattle, WA 98124

Mr. M. E. Wilke, Chief Engineer
Burgess Division
Gould, Inc.
Freeport, IL 61032

Dr. Eugene Willihnganz
C & D Batteries
Division of ELTRA Corporation
3043 Walton Road
Plymouth Meeting, PA 19462

Professor T. P. Dirkse
Calvin College
3175 Burton Street, S.E.
Grand Rapids, MI 49506

Mr. F. Tepper
Catalyst Research Corporation
6101 Falls Road
Baltimore, MD 21209

Mr. C. E. Thomas
Chrysler Corporation
Space Division
P. O. Box 29200
New Orleans, LA 70129

Dr. L. J. Minnich
G. & W. H. Corson, Inc.
Plymouth Meeting, PA 19462

Mr. J. A. Keralla
Delco Remy Division
General Motors Corporation
2401 Columbus Avenue
Anderson, IN 46011

Mr. J. M. Williams
Experimental Station, Bldg. 304
Engineering Materials Laboratory
E. I. duPont de Nemours & Company
Wilmington, Delaware 19898

Dr. A. Salkind
ESB, Inc. Research Center
19 West College Avenue
Yardley, PA 19067

Mr. E. P. Broglio
Eagle-Picher Industries, Inc.
P. O. Box 47, Couples Dept.
Joplin, MO 64801

Mr. V. L. Best
Elpower Corporation
2117 South Anne Street
Santa Ana, CA 92704

Dr. W. P. Cadogan
Emhart Corporation
Box 1620
Hartford, CT 06102

Dr. H. G. Oswin
Energetics Science, Inc.
4461 Bronx Blvd.
New York, NY 10470

Mr. Martin Klein
Energy Research Corporation
15 Durant Avenue
Bethel, CT 06801

Dr. Arthur Fleischer
466 South Center Street
Orange, NJ 07050

Dr. R. P. Hamlen
Research and Development Center
General Electric Company
P. O. Box 43, Bldg., 37
Schenectady, NY 12301

Mr. Kenneth Hanson
General Electric Company
Valley Forge Space Technology Center
P. O. Box 8555
Philadelphia, PA 19101

Distribution List (Cont.)

Mr. Aaron Kirpich
Space Systems, Room M2614
General Electric Company
P. O. Box 8555
Philadelphia, PA 19101

Mr. P. R. Voyentzie
Battery Products Section
General Electric Company
P. O. Box 114
Gainsville, FL 32601

Mr. David F. Schmidt
General Electric Company
777 14th Street, N. W.
Washington, DC 20005

Dr. R. Goodman
Globe-Union, Inc.
P. O. Box 591
Milwaukee, WI 50201

Dr. J. E. Oxley
Gould Ionics, Inc.
P. O. Box 3140
St. Paul, Minnesota 55165

Grumman Aerospace Corporation
S. J. Gaston, Plant 35, Dept. 567
Bethpage, Long Island
New York 11714

Battery and Power Sources Division
Gulton Industries
212 Durham Avenue
Metuchen, NJ 08840

Dr. P. L. Howard
Centreville, MD 21617

Dr. M. E. Ellion, Manager,
Propulsion & Power Systems Lab.
Building 366, MS 524
Hughes Aircraft Company
El Segundo, CA 90245

Mr. R. Hamilton
Institute for Defense Analyses
400 Army-Navy Drive
Arlington, VA 22202

Dr. R. Briceland
Institute for Defense Analyses
400 Army-Navy Drive
Arlington, VA 22202

Mr. N. A. Matthews
International Nickel Company
1000-16th Street, N.W.
Washington, DC 20036

Dr. Richard E. Evans
Applied Physics Laboratory
Johns Hopkins University
8621 Georgia Avenue
Silver Spring, MD 20910

Dr. A. Moos
Leesona Moos Laboratories
Lake Success Park, Community Drive
Great Neck, NY 11021

Dr. R. A. Wynveen, President
Life Systems, Inc.
23715 Mercantile Road
Cleveland, OH 44122

Dr. James D. Birkett
Arthur D. Little, Inc.
Acorn Park
Cambridge, MA 02140

Mr. Robert E. Corbett
Department 62-25, Building 151
Lockheed Aircraft Corporation
P. O. Box 504
Sunnyvale, CA 94088

Mr. S. J. Angelovich
Chief Engineer
Mallory Battery Company
South Broadway
Tarrytown, NY 10591

Dr. Per Bro
P. R. Mallory & Company, Inc.
Library
Northwest Industrial Park
Burlington, MA 01801

P. R. Mallory & Company, Inc.
Library
P. O. Box 1115
Indianapolis, IN 46206

Messrs. William B. Collins and
M. S. Imamura
Martin-Marietta Corporation
P. O. Box 179
Denver, CO 80201

Distribution List (Cont.)

Mr. A. D. Tonelli, MS 17, Bldg. 22
A3-830
McDonnell Douglas Astronautics Co.
5301 Bolsa Avenue
Huntington Beach, CA 92647

Dr. Robert C. Shair
Motorola, Inc.
8000 W. Sunrise Blvd.
Ft. Lauderdale, FL 33313

Rocketdyne Division
North American Rockwell Corporation
Attn: Library
6633 Canoga Avenue
Canoga Park, CA 91304

Mr. D. C. Briggs
WDL Division
Philco-Ford Corporation
3939 Fabian Way
Palo Alto, CA 94303

Power Information Center
University City Science Institute
3401 Market Street, Room 2210
Philadelphia, PA 19014

RAI Research Corporation
225 Marcus Blvd
Hauppauge, L. I., NY 11787

Southwest Research Institute
Attn: Library
P. O. Drawer 28510
San Antonio, TX 78228

Mr. Joseph M. Sherfey
5261 Nautilus Drive
Cape Coral, FL 33904

Dr. W. R. Scott (M-2/2154)
TRW Systems, Inc.
One Space Park
Redondo Beach, CA 90278

Dr. Herbert P. Silverman (R-1/2094)
TRW Systems, Inc.
One Space Park
Redondo Beach, CA 90278

TRW, Inc.
Attn: Librarian TIM 3417
23555 Euclid Avenue
Cleveland, OH 44117

Union Carbide Corporation
Development Laboratory Library
P. O. Box 6056
Cleveland, OH 44101

Dr. Robert Powers
Consumer Products Division
Union Carbide Corporation
P. O. Box 6116
Cleveland, OH 44101

Dr. C. C. Hein, Contract Admin.
Research and Development Center
Westinghouse Electric Corporation
Churchill Borough
Pittsburgh, PA 15235

Yardney Electric Corporation
Power Sources Division
3850 Olive Street
Denver, CO 80207

Yardney Electric Division
82 Mechanic Street
Pawcatuck, CT 02891

Dr. Charles Levine
Dow Chemical U.S.A.
Walnut Creek Research Center
2800 Mitchell Drive
Walnut Creek, CA 94598

Prof. Donald M. Smyth
Materials Research Center
Lehigh University
Bethlehem, PA 18015

Prof. John W. Patterson
Dept. of Metallurgy
Iowa State University
Ames, IA 50010

Prof. Rustum Roy
Materials Science Dept.
Pennsylvania State University
University Park, PA 16802

Prof. John H. Kennedy
Univ. of Calif. at Stanta Barbara
Santa Barbara, CA 93106

Dr. Paul Jorgensen
Stanford Research Institute
Menlo Park, CA 94025

Distribution List (Cont.)

Dr. L. Topper
Division of Advanced Technology
Applications
National Sciences Foundation
Washington, DC 20550

Mr. L. R. Rothrock
Union Carbide Corp.
8888 Balboa Ave
San Diego, CA 92123

Dr. Robert A. Huggins
Dept. of Materials Science
and Engineering
Stanford University
Stanford, CA 94305

Dr. M. Stanley Whittingham
Esso Research and Engineering Co.
Linden, NJ 07036

Dr. Neill T. Weber
Ford Motor Co. Research Lab
Dearborn, MI 48121

Prof. James I. Mueller
Ceramic Engineering Div.
University of Washington
Seattle, WA 98195

Dr. Douglas O. Raleigh
North American Rockwell
Science Center
Thousand Oaks, CA 91360

Dr. R. H. Doremus
Rensselaer Polytechnic Institute
Materials Division
Troy, NY 12181

Dr. Robert S. Roth
National Bureau of Standards
U. S. Department of Commerce
Washington, DC 20234

Prof. Alexander F. Wells
Dept. of Chemistry
University of Connecticut
Storrs, CT 06268